https://doi.org/10.1016/j.jfranklin.2023.03.001

On the dynamics of a quantum coherent feedback network of cavity-mediated double quantum dot qubits

Zhiyuan Dong[a], Wei Cui[b,c], Guofeng Zhang[d,e,*]

[a] *School of Science, Harbin Institute of Technology, Shenzhen, China*
[b] *School of Automation Science and Engineering, South China University of Technology, Guangzhou, China*
[c] *Pazhou Laboratory, Guangzhou, 510330, China*
[d] *Department of Applied Mathematics, The Hong Kong Polytechnic University, Hung Hom, Hong Kong*
[e] *The Hong Kong Polytechnic University Shenzhen Research Institute, Shenzhen, 518057, China*

Abstract

The purpose of this paper is to present a comprehensive study of a coherent feedback network where the main component consists of two distant double quantum dot (DQD) qubits which are directly coupled to a cavity. This main component has recently been physically realized (van Woerkom *et al.*, Microwave photon-mediated interactions between semiconductor qubits, Physical Review X, 8(4):041018, 2018). The feedback loop is closed by cascading this main component with a beamsplitter. The dynamics of this coherent feedback network is studied from three perspectives. First, an analytic form of the output single-photon state of the network driven by a single-photon state is derived. In contrast to the experimental observations made in the above paper where a laser is used as input, new interesting physical phenomena are revealed by means of single-photon input. Second, excitation probabilities of DQD qubits are computed when the network is driven by a single-photon input state. Finally, if the input is vacuum but one of the two DQD qubits is initialized in its excited state, the explicit expression of the steady-state joint system-field state is derived, which shows that the output single-photon field and the two DQD qubits can form an entangled state if the transition frequencies of two DQD qubits are equal. This analytical expression can be used to interpret experimental results in the existing literature.

Keywords: Single-photon state, double quantum dot (DQD) qubit, quantum coherent feedback network, quantum control, open quantum systems.

1. Introduction

In the past few decades, quantum control has attracted much attention due to the rapid development of quantum information science and technology. Efficient manipulation of the interaction between photons (flying qubits) and finite-level quantum systems (stationary qubits) is necessary for quantum control which enables quantum communication [1], quantum network [2], quantum filtering [3] and quantum learning control [4]. With the advancement of technology in quantum optics and solid-state devices physics, the ultrastrong coupling regime of quantum light-matter interaction is currently an active research field [5, 6, 7]. The interaction between a DQD qubit and a nearby quantum point contact (QPC) is investigated in [8, 9].

*Corresponding author.
Email address: guofeng.zhang@polyu.edu.hk (Guofeng Zhang)
URL: https://www.polyu.edu.hk/ama/profile/gfzhang (Guofeng Zhang)

Particularly, Lyapunov-based control method is used in [8] to transfer the charge qubit to its target state. In [9], the master equation for a DQD qubit is derived and the measurement-induced backaction is considered. Moreover, a Hamiltonian feedback control law is proposed to stabilize a particular tunneling current and realize its convergence to the target value.

As flying qubits, single photons are a promising candidate for quantum information processing. For example, the strong nonlinear interaction between photons and optical emitters can be used to engineer a single-photon transistor [10]. The operation principle of the single-photon transistor is to use either zero or one photon in the storage step, then the subsequent transmitted or reflected photons are controlled by the conditional flip of the "gate" pulse. Another single-photon transistor is introduced in [11] to setup a circuit quantum electrodynamical (circuit QED) model, which consists of two two-level systems. Although no photons are exchanged between the two transmission lines in this circuit, one photon can completely block or enable the propagation of the other by the interaction between the two two-level systems. Recently, the realization of an optical transistor is given in [12], which consists of a four-level system and a stored photon to control the transmission of source photons.

From a control-theoretic point of view, analysis of quantum systems' response to single-photon states is an essential aspect of control systems engineering. The interaction of quantum systems with single-photon states has been extensively studied in recent years, see e.g., [13, 14, 15, 16, 17, 18, 19]. The transmission and reflection probabilities in terms of the stationary output photon state are discussed by using the scattering matrix [13, 14, 15]. In [17], an analytical expression of the output field state is derived for a class of quantum finite-level systems driven by single-photon input states. Interestingly, it is shown that quantum linear systems theory [16, 20, 21] can be adopted to derive the pulse shapes of the output single-photon states. On the other hand, the problem of quantum filtering for systems driven by single-photon states has been attracting growing interest due to their promising applications in quantum communication and measurement feedback control, see e.g., [22, 23, 24, 25, 26, 27, 28, 29] and references therein.

Recently, the microwave photon-mediated interactions between semiconductor qubits have been physically implemented by quite a few experimental platforms [30, 31, 32], including superconducting circuits [33, 34, 35], NV spin ensembles [36], and double quantum dots [37, 38, 39]. As pointed out by these references, strong coupling regimes of light-matter interaction and the corresponding generated multipartite entangled states are crucial for numerous applications in quantum information science. In this paper, two double quantum dots (DQDs) are modeled as two charge qubits. These two DQD qubits are separated from one another; however they are both directly coupled to a microwave cavity. In other words, the cavity enables information exchange between the *distant* DQD qubits. Indeed, this is a class of Tavis-Cummings system and we are interested in its dynamics when it is driven by a single photon. For easy reference, this system is called the coupled system G in our paper. Moreover, we cascade a beamsplitter with G to form a quantum coherent feedback network as shown in Fig. 1 in Section 3, and aim to study the dynamics of this coherent feedback network. The interesting phenomena observed in light-matter interacting experiments, such as the dark states, vacuum Rabi oscillation, the entangled states, have been theoretical analyzed with the aid of control theory. In contrast to the laser input considered in the references, a continuous-mode single-photon Fock state is used as the input of the coherent feedback network, which is more realistic and with general applicability.

The rest of this paper is organized as follows. Some preliminaries are summarized in Section 2, which

include notation to be used, open quantum systems and single-photon states. The quantum coherent feedback network is presented in Section 3. The steady-state output field state of the coherent feedback network driven by a single-photon input is derived in Section 4. Section 5 presents the master equations for the 1st DQD qubit and discusses the changes of excitation probability with various system parameters. An analytical expression of the joint system-field state is given in Section 6, which shows the entanglement between a free-propagating single photon and the two DQD qubits. Section 7 concludes this paper.

2. Preliminaries

In this section, we introduce the notation to be used in this paper. A concise introduction to open Markovian quantum systems and continuous-mode single-photon states is also given.

Notation. Let $i = \sqrt{-1}$ be the imaginary unit and $|\Phi_0\rangle$ the vacuum state of a free-propagating field. Given a column vector of complex numbers or operators $X = [x_1, \cdots, x_n]^\top$, the complex conjugate or adjoint operator of X is denoted by $X^\# = [x_1^*, \cdots, x_n^*]^\top$. Let $X^\dagger = (X^\#)^\top$. Clearly, when $n = 1$, $X^\dagger = X^*$. $[A, B] = AB - BA$ denotes the commutator between operators A and B. Define two superoperators as

$$\begin{aligned} &\text{Lindbladian} : \mathcal{L}_G X \triangleq -i[X, H] + \mathcal{D}_L X, \\ &\text{Liouvillian} : \mathcal{L}_G^\star \rho \triangleq -i[H, \rho] + \mathcal{D}_L^\star \rho, \end{aligned} \tag{1}$$

where $\mathcal{D}_A B = A^\dagger B A - \frac{1}{2}(A^\dagger A B + B A^\dagger A)$ and $\mathcal{D}_A^\star B = A B A^\dagger - \frac{1}{2}(A^\dagger A B + B A^\dagger A)$. We have $\mathrm{Tr}[\rho \mathcal{L}_G X] = \mathrm{Tr}[X \mathcal{L}_G^* \rho]$ for a density operator ρ and a bounded operator X. Finally, $\otimes$ denotes the tensor product, and the tensor product $|\phi\rangle \otimes |\psi\rangle$ is often shorthanded as $|\phi\psi\rangle$ in this paper.

2.1. System and field

Open Markovian quantum systems can be parameterized conveniently by the (S, L, H) formalism [40, 41, 42, 24, 43, 44]. To be specific, for a quantum system driven by free-propagating Boson fields, S is a unitary operator for example a phase shifter or beamsplitter. The coupling between the system and the fields is described by the operator L, and the self-adjoint operator H is the initial system Hamiltonian. S, L, H are all operators on the system Hilbert space $\mathcal{H}_S$. A free-propagating field is described by its annihilation operator $b(t)$ and creation operator $b^\dagger(t)$ (the adjoint of $b(t)$), which are operators on a Fock space $\mathcal{H}_F$ and satisfy the following properties

$$\begin{aligned} &b(t)\,|\Phi_0\rangle = 0, \quad [b(t), b(r)] = [b^\dagger(t), b^\dagger(r)] = 0, \\ &[b(t), b^\dagger(r)] = \delta(t - r), \quad \forall t, r \in \mathbb{R}. \end{aligned} \tag{2}$$

The integrated annihilation operator and creation operator are defined as $B(t) = \int_{t_0}^t b(s) ds$ and $B^\dagger(t) = \int_{t_0}^t b^\dagger(s) ds$, respectively, where t_0 is the initial time, namely, the time when the system and field start interaction.

An open quantum system exchanges energy/information with its environment — the free-propagating Boson fields. Assuming $S = I$ (the identity operator), the dynamical evolution of the total system (the system of interest plus fields) can be described by a unitary operator $U(t, t_0)$ on the tensor product Hilbert

space $\mathcal{H}_S \otimes \mathcal{H}_F$, which is the solution to the following quantum stochastic differential equation (QSDE) [45, 3, 41, 46, 17, 47]

$$dU(t,t_0) = \left\{ -\left(\frac{1}{2}L^\dagger L + iH\right)dt + LdB^\dagger(t) - L^\dagger dB(t)\right\}U(t,t_0), \quad t \geq t_0 \tag{3}$$

with the initial condition $U(t_0,t_0) = I$. Let $|\Psi(t)\rangle$ be the joint system-field state (wavefunction) at time $t \geq t_0$. Then in the Schrödinger picture it is well-known that

$$|\Psi(t)\rangle = U(t,t_0)\,|\Psi(t_0)\rangle\,. \tag{4}$$

On the other hand, we can also study the dynamics of the system in the Heisenberg picture. Based on (3), the time evolution of a system operator X on $\mathcal{H}_S$, defined as

$$j_t(X) \equiv X(t) \triangleq U^\dagger(t)(X \otimes I)U(t), \tag{5}$$

is given by [3, 41, 46, 17]

$$dj_t(X) = j_t(\mathcal{L}_G X)dt + j_t([L^\dagger, X])dB(t) + j_t([X, L])dB^\dagger(t). \tag{6}$$

As terms $dB(t)$ and $dB^\dagger(t)$ are involved in the time evolution of $j_t(X)$, it is an operator on the tensor product Hilbert space $\mathcal{H}_S \otimes \mathcal{H}_F$. In this way, the system takes information from the input fields. After system-field interaction, an output field is generated, which in the input-output formalism is given by [3, 41, 46, 17]

$$dB_{\rm out}(t) = L(t)dt + dB(t), \tag{7}$$

where $B_{\rm out}(t) = U^\dagger(I \otimes B(t))U(t)$ denotes the integrated output annihilation operator. Clearly, $B_{\rm out}(t)$ is an operator on the tensor product Hilbert space $\mathcal{H}_S \otimes \mathcal{H}_F$. Thus, the output fields carry the system's information which can be measured. More discussions on open quantum systems can be found in, e.g. [48, 49, 50, 51, 52, 53, 26, 54].

2.2. Continuous-mode single-photon state

A continuous-mode single-photon state in the time domain can be defined as

$$|\Phi_1\rangle \triangleq B^\dagger(\xi)\,|\Phi_0\rangle\,, \tag{8}$$

where $\xi(t)$ is the temporal pulse shape which satisfies $\|\xi\| \triangleq \sqrt{\int_{-\infty}^{\infty} |\xi(t)|^2 dt} = 1$, and

$$B^\dagger(\xi) \triangleq \int_{-\infty}^{\infty} \xi(t) b^\dagger(t) dt. \tag{9}$$

Simply speaking, (8) means that a photon is generated at time t by the creation operator $b^\dagger(t)$ from the vacuum $|\Phi_0\rangle$ with probability $|\xi(t)|^2$, thus the normalization condition $\|\xi\| = 1$ guarantees that exactly one photon is generated. Fourier transforming (8), yields the continuous-mode single-photon state in the frequency domain,

$$|\Phi_1\rangle = \int_{-\infty}^{\infty} \xi[i\omega] b^\dagger[i\omega] d\omega\,|\Phi_0\rangle\,, \tag{10}$$

where square brackets are used to indicate that the designated operators or functions are in the frequency domain. Generally speaking, the continuous-mode single-photon state $|\Phi_1\rangle$ in (10) describes a single photon which is coherently superposed over a continuum of frequency modes, with probability amplitudes given by the spectral density function $\xi[i\omega]$. In other words, the probability of finding the photon in the frequency interval $[\omega, \omega + d\omega)$ is $|\xi[i\omega]|^2$, or equivalently, the probability of finding the photon in the time interval $[t, t + dt)$ is $|\xi(t)|^2$. More discussions on single-photon states can be found in, e.g., [55, 14, 56].

3. Coherent feedback network

In this paper we focus our sight on the dynamics of the quantum coherent feedback network as shown in Fig. 1. In this section, we describe the mathematical model.

The coupled system G consists of two DQD qubits which are directly coupled to a microwave cavity. The system G has been recently physically implemented in a semiconductor platform [38]. It is worthwhile to notice that the two DQD qubits are separated from each other, thus their interaction is mediated by the microwave cavity which plays the role of a bus. In this paper, we add a beamsplitter which cascades with G, thus forming a coherent feedback network with input b_0 and output b_3.

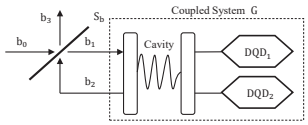

Figure 1: Schematic of the coherent feedback network.

In the (S, L, H) formalism, the beamsplitter $\mathbf{S_b}$ in Fig. 1 has parameters $(S_b, 0, 0)$, where

$$S_b = \begin{bmatrix} \mu & \sqrt{1-\mu^2} \\ \sqrt{1-\mu^2} & -\mu \end{bmatrix} \tag{11}$$

with μ being the reflection parameter ($0 \leq \mu < 1$). Each of these two DQDs is in the Coulomb-blockade regime with strong intradot and interdot interaction, and spanned by two basis states $|0\rangle = |1, 0\rangle$ and $|1\rangle = |0, 1\rangle$. With further transformation, each DQD has a ground state $|g\rangle = \alpha\,|0\rangle - \beta\,|1\rangle$ and an excited state $|e\rangle = \beta\,|0\rangle + \alpha\,|1\rangle$, where α and β represent the relationship between the coupling strength and the energy offset. In this paper, a DQD qubit has a Hamiltonian of the form

$$H_{\mathrm{DQD}} = \frac{\omega_0}{2}\sigma_z, \tag{12}$$

where $\sigma_z = |e\rangle\langle e| - |g\rangle\langle g|$ is a Pauli matrix, and ω_0 is the transition frequency between $|g\rangle$ and $|e\rangle$, which is typically around 5 GHz [38, 7]. It should be noted that the transition frequency ω_0 is normalized as unit 1 throughout this paper. The two DQD qubits in Fig. 1 are expressed with the (S, L, H) parameters

$$(S_{\mathrm{DQD}_k}, L_{\mathrm{DQD}_k}, H_{\mathrm{DQD}_k}) = (-, -, \frac{1}{2}\delta\omega_k\sigma_{z,k}), \quad k = 1, 2, \tag{13}$$

where $\delta\omega_k = \omega_k - \omega_p$ ($k = 1, 2$) is the detuning between the transition frequency ω_k of the kth DQD qubit and the carrier frequency ω_p of the input field. Moreover, $\delta\omega_k > 0$ means the red detuning, while the blue

detuning is effected by $\delta\omega_k < 0$. As the DQD qubits are directly coupled to the cavity, instead of fields, they have no S and L parameters. Under the rotating-wave approximation (RWA), the Hamiltonian of the coupled system G is

$$H_{\rm sys} = \delta\omega_r a^\dagger a + \frac{1}{2}\sum_{k=1}^{2}\delta\omega_k\sigma_{z,k} + \sum_{k=1}^{2} g_k \sin\theta_k(\sigma_{-,k}a^\dagger + \sigma_{+,k}a), \tag{14}$$

where $\delta\omega_r$ is the frequency detuning between the cavity resonance frequency and the carrier frequency of the input field, and $\sigma_- = |g\rangle\langle e|$, $\sigma_+ = |e\rangle\langle g|$ are the lowering and raising operators of the DQD qubit. The third term in (14) models the direct coupling between the two DQD qubits and the cavity. (A more detailed description of direct coupling between quantum systems can be found in [57, 24]). The microwave cavity is lossy, in other words, it exchanges energy with its environment. Let its coupling strength be denoted by κ. Then, in the (S, L, H) formalism, the coupled system G is parameterized as

$$(S_{\rm sys}, L_{\rm sys}, H_{\rm sys}) = \left(1, \sqrt{\kappa}a, \delta\omega_r a^\dagger a + \frac{1}{2}\sum_{k=1}^{2}\delta\omega_k\sigma_{z,k} + \sum_{k=1}^{2} g_k \sin\theta_k(\sigma_{-,k}a^\dagger + \sigma_{+,k}a)\right). \tag{15}$$

Remark 3.1. *The coupled system G has recently been physically implemented on a semiconducting platform [38]. The system Hamiltonian $H_{\rm sys}$ in* (15) *is the same as that in [38, (C7)]. The system G studied in [38] is driven by a laser which is modelled as a coherent state with amplitude α. In this paper, the input is either the vacuum or a continuous-mode single-photon state, in both these two cases $\alpha = 0$. As a result, the coupling operator in [38, (C13)] reduces to $\sqrt{\kappa_{\rm ext}}a$, which is $L_{\rm sys}$ in* (15) *where κ is used instead of $\kappa_{\rm ext}$. Finally, the nonradiative losses and dephasing processes are neglected in this paper. An interested reader may refer to [38] for more details of the physics and practical implementation of the coupled system G. It should be noted that the decoherence of the DQD qubits has been ignored, since we focus on the dynamic analysis of the quantum feedback network. Finally, for notational simplicity, we denote the coupling strength $g_k \sin\theta_k$ by Γ_k in the remainder of this paper.*

By means of the (S, L, H) parameters in (15), the QSDEs for the system G in the Heisenberg picture in the rotating frame are

$$\begin{aligned}\begin{bmatrix}\dot\sigma_{-,1}\\ \dot\sigma_{-,2}\\ \dot a\end{bmatrix} &= \begin{bmatrix}-i\delta\omega_1 & 0 & i\Gamma_1\sigma_{z,1}\\ 0 & -i\delta\omega_2 & i\Gamma_2\sigma_{z,2}\\ -i\Gamma_1 & -i\Gamma_2 & -i\delta\omega_r - \frac{\kappa}{2}\end{bmatrix}\begin{bmatrix}\sigma_{-,1}\\ \sigma_{-,2}\\ a\end{bmatrix} - \begin{bmatrix}0\\ 0\\ \sqrt{\kappa}\end{bmatrix} b_1,\\ b_2 &= \sqrt{\kappa}a + b_1.\end{aligned} \tag{16}$$

Clearly, (16) is a bilinear system. Let the coupled system G be initialized in the state $|g_1\rangle \otimes |g_2\rangle \otimes |0\rangle$; in other words, the two DQD qubits are in their ground states and the cavity is empty. Moreover, let the input field b_1 to the coupled system G be in the vacuum state $|\Phi_0\rangle$. Denote

$$|\Phi\rangle = |\eta\rangle \otimes |\Phi_0\rangle, \tag{17}$$

where $|\eta\rangle = |g_1\rangle\otimes|g_2\rangle\otimes|0\rangle$ is the initial state of the coupled system G, and $X(t) = [\ \sigma_{-,1}(t) \quad \sigma_{-,2}(t) \quad a(t)\ ]^T$. Then, following the proofs of Lemma 3 and Theorem 5 in [17], it can be shown that

$$\begin{aligned}\langle\Phi|\dot X(t) &= A\langle\Phi|X(t) + B\langle\Phi|b_1(t),\\ b_2(t) &= CX(t) + b_1(t),\end{aligned} \tag{18}$$

where $B = [\ 0 \quad 0 \quad -\sqrt{\kappa}\ ]^T$, $C = -B^T$, and

$$A = \begin{bmatrix} -i\delta\omega_1 & 0 & -i\Gamma_1 \\ 0 & -i\delta\omega_2 & -i\Gamma_2 \\ -i\Gamma_1 & -i\Gamma_2 & -i\delta\omega_r - \frac{\kappa}{2} \end{bmatrix}. \tag{19}$$

Next, we look at the closed-loop system. The beamsplitter $\mathbf{S_b}$ in Fig. 1 is a static system,

$$\begin{bmatrix} b_3 \\ b_1 \end{bmatrix} = S_b \begin{bmatrix} b_0 \\ b_2 \end{bmatrix}. \tag{20}$$

By the linear fractional transform [24, Section 4.4], the coherent feedback network in Fig. 1 can be expressed in the (S, L, H) formalism as

$$(S_{\text{total}}, L_{\text{total}}, H_{\text{total}}) = \left(1, \sqrt{\frac{1-\mu}{1+\mu}} L_{\text{sys}}, H_{\text{sys}}\right). \tag{21}$$

Remark 3.2. *By comparing the (S, L, H) parameters (21) of the quantum coherent feedback network and (15) of the coupled system G, it can be seen that only the coupling operator is changed. More specifically, κ is replaced with $\tilde{\kappa} \triangleq \frac{1-\mu}{1+\mu}\kappa$. Thus, the coupling strength between the coupled system G and the input field, which is the decay rate of the cavity, can be tuned by changing the beamsplitter reflection parameter μ. Clearly, the coherent feedback network reduces to the open-loop coupled system G when $\mu = 0$.*

By (21), only the coupling strength is changed by the beamsplitter. As a result, similar to (18), the QSDEs for the quantum coherent feedback network acting on $\langle\Phi|$ are

$$\begin{aligned} \langle\Phi|\dot{X}(t) &= \tilde{A}\langle\Phi|X(t) + \tilde{B}\langle\Phi|b_0(t), \\ b_3(t) &= \tilde{C}X(t) + b_0(t), \end{aligned} \tag{22}$$

where

$$\begin{aligned} \tilde{A} &= \begin{bmatrix} -i\delta\omega_1 & 0 & -i\Gamma_1 \\ 0 & -i\delta\omega_2 & -i\Gamma_2 \\ -i\Gamma_1 & -i\Gamma_2 & -i\delta\omega_r - \frac{\tilde{\kappa}}{2} \end{bmatrix}, \\ \tilde{B} &= \begin{bmatrix} 0 & 0 & -\sqrt{\tilde{\kappa}} \end{bmatrix}^T, \quad \tilde{C} = -\tilde{B}^T. \end{aligned} \tag{23}$$

(Recall that $\tilde{\kappa} = \frac{1-\mu}{1+\mu}\kappa$ as defined in Remark 3.2.) System (22) is of the form of a linear quantum system. By linear systems theory ([16, 53, 17]) we get

$$\langle\Phi|\, b_3(t) = \tilde{C}e^{\tilde{A}(t-t_0)}\, \langle\Phi|\, X(t_0) + \int_{t_0}^{t} g_{\tilde{G}}(t-\tau)\, \langle\Phi|\, b_0(\tau)d\tau, \tag{24}$$

where the impulse response function $g_{\tilde{G}}(t)$ is given by

$$g_{\tilde{G}}(t) = \begin{cases} \delta(t) + \tilde{C}e^{\tilde{A}t}\tilde{B}, & t \geq 0, \\ 0, & t < 0, \end{cases} \tag{25}$$

whose corresponding transfer function is

$$\tilde{G}[s] = \frac{\Gamma_1^2(s+i\delta\omega_2) + \Gamma_2^2(s+i\delta\omega_1) + (s+i\delta\omega_1)(s+i\delta\omega_2)(s+i\delta\omega_r - \frac{\tilde{\kappa}}{2})}{\Gamma_1^2(s+i\delta\omega_2) + \Gamma_2^2(s+i\delta\omega_1) + (s+i\delta\omega_1)(s+i\delta\omega_2)(s+i\delta\omega_r + \frac{\tilde{\kappa}}{2})}. \tag{26}$$

It can be verified that $\tilde{G}[s]$ is an all-pass filter, which only modulates the phase of the input light. It can be easily seen that the coupled system G is an all-pass filter too. The following lemma presents the stability condition of the quantum feedback network.

Lemma 3.1. *All the eigenvalues of the matrix $\tilde{A}$ have non-positive real part. Moreover, the matrix $\tilde{A}$ is marginally stable if and only if $\delta\omega_1 = \delta\omega_2$.*

Proof. Firstly, as the eigenvalues of the matrix $\tilde{A}+\tilde{A}^\dagger$ are $\{0,\ 0,\ -\tilde{\kappa}\}$, all the eigenvalues of the matrix $\tilde{A}$ have non-positive real part. In what follows, we show that the matrix $\tilde{A}$ is marginally stable if and only if $\delta\omega_1 = \delta\omega_2$. Let λ be an eigenvalue of the matrix $\tilde{A}$. Then the characteristic polynomial equation is

$$\lambda^3 + (p_1 + q_1 i)\lambda^2 + (p_2 + q_2 i)\lambda + (p_3 + q_3 i) = 0, \tag{27}$$

where

$$\begin{aligned}
p_1 &= \frac{\tilde{\kappa}}{2},\\
q_1 &= \delta\omega_r + \delta\omega_1 + \delta\omega_2,\\
p_2 &= \Gamma_1^2 + \Gamma_2^2 - \delta\omega_1\delta\omega_2 - \delta\omega_1\delta\omega_r - \delta\omega_2\delta\omega_r,\\
q_2 &= \frac{\tilde{\kappa}}{2}(\delta\omega_1 + \delta\omega_2),\\
p_3 &= -\frac{\tilde{\kappa}}{2}\delta\omega_1\delta\omega_2,\\
q_3 &= \Gamma_1^2\delta\omega_2 + \Gamma_2^2\delta\omega_1 - \delta\omega_1\delta\omega_2\delta\omega_r.
\end{aligned} \tag{28}$$

The generalized Hurwitz matrix [58] is given by

$$M = \begin{bmatrix}
p_1 & q_2 i & p_3 & 0 & 0 & 0\\
1 & q_1 i & p_2 & q_3 i & 0 & 0\\
0 & p_1 & q_2 i & p_3 & 0 & 0\\
0 & 1 & q_1 i & p_2 & q_3 i & 0\\
0 & 0 & p_1 & q_2 i & p_3 & 0\\
0 & 0 & 1 & q_1 i & p_2 & q_3 i
\end{bmatrix}. \tag{29}$$

Let Δ_j be the jth order determinant of M, $j = 1, \ldots, 6$. Then the Routh like table [58] gives

$$R_1 = 1,\ R_2 = p_1,\ R_j = \frac{\Delta_{j-1}}{\Delta_{j-2}},\ j = 3, \ldots, 6. \tag{30}$$

All the three pairs of points $P_1(R_1, R_2)$, $P_2(R_3, R_4)$, $P_3(R_5, R_6)$ have the same signs (R_3 and R_4 are pure imaginary) is equivalent to

$$R_1 R_2 > 0,\ R_3 R_4 < 0,\ R_5 R_6 > 0, \tag{31}$$

which is equivalent to $\delta\omega_1 \neq \delta\omega_2$. Consequently, according to the Sign Pair Criterion (SPC) [58], all the eigenvalues λ_i of the matrix $\tilde{A}$ are in the L.H.S. of the complex plane if and only if $\delta\omega_1 \neq \delta\omega_2$. Thus, the matrix $\tilde{A}$ is marginally stable if and only if $\delta\omega_1 = \delta\omega_2$.

When $\delta\omega_1 = \delta\omega_2 = \delta\omega_s$ for some $\delta\omega_s \in \mathbb{R}$, the system matrix $\tilde{A}$ in (23) can be factorized as

$$\tilde{A} = V^{-1}\Lambda_s V, \tag{32}$$

where $\Lambda_s = \text{diag}\{\lambda_1\ , \lambda_2,\ \lambda_3\}$ with the corresponding eigenvalues

$$\begin{aligned}
\lambda_1 &= -i\delta\omega_s, \\
\lambda_2 &= -\frac{1}{4}\left[\tilde{\kappa} + 2i(\delta\omega_r + \delta\omega_s)\right] - \lambda', \\
\lambda_3 &= -\frac{1}{4}\left[\tilde{\kappa} + 2i(\delta\omega_r + \delta\omega_s)\right] + \lambda',
\end{aligned} \tag{33}$$

and

$$\lambda' = \frac{1}{4}\sqrt{[\tilde{\kappa} + 2i(\delta\omega_r - \delta\omega_s)]^2 - 16(\Gamma_1^2 + \Gamma_2^2)}. \tag{34}$$

In particular, the eigenvector associated with the imaginary eigenvalue $\lambda_1 = -i\delta\omega_s$ is of the form

$$x = \varpi \left(\Gamma_2 \begin{bmatrix} 1 \\ 0 \\ 0 \end{bmatrix} - \Gamma_1 \begin{bmatrix} 0 \\ 1 \\ 0 \end{bmatrix} + 0 \begin{bmatrix} 0 \\ 0 \\ 1 \end{bmatrix} \right), \tag{35}$$

where ϖ is an arbitrary non-zero number. Moreover, in this case, the transfer function $\tilde{G}[s]$ in (26) reduces to

$$\tilde{G}[s] = \frac{\Gamma_1^2 + \Gamma_2^2 + (s + i\delta\omega_s)(s + i\delta\omega_r - \frac{\tilde{\kappa}}{2})}{\Gamma_1^2 + \Gamma_2^2 + (s + i\delta\omega_s)(s + i\delta\omega_r + \frac{\tilde{\kappa}}{2})}. \tag{36}$$

Remark 3.3. *It is worthwhile to notice that equations in* (22) *are the QSDEs for a passive linear quantum system with system Hamiltonian* $\delta\omega_r a^\dagger a + \frac{1}{2}\sum_{k=1}^2 \delta\omega_k a_k^\dagger a_k + \sum_{k=1}^2 \Gamma_k(a_k a^\dagger + a_k^\dagger a)$ *with* a_1 *and* a_2 *being annihilation operators, and* S_{total} *and* L_{total} *are the same as those in* (21)*. More interestingly, when* $\delta\omega_1 = \delta\omega_2 = \delta\omega_s$*, this quantum passive linear system has an imaginary pole* $-i\delta\omega_s$ *and an associated eigenstate given in* (35)*. By [59, Theorem 3.2], this eigenstate spans a subsystem which is uncontrollable and unobservable, i.e. a decoherence-free subsystem (DFS). In fact, this DFS is for the system operator* $\Gamma_2 a_1 - \Gamma_1 a_2$*, a special combination of* a_1 *and* a_2*. It can be verified that this particular combination of* a_1 *and* a_2 *is neither reachable by an input nor detectable by an output. More discussions on DFSs of quantum linear systems can be found in [60, 61, 59] and references therein.*

Remark 3.4. *Comparing* (26) *and* (36)*, it can be been that when* $\delta\omega_1 = \delta\omega_2 = \delta\omega_s$*, the common factor* $s + i\delta\omega_s$ *of the numerator and denominator is cancelled. Notice that this common factor gives rise to the imaginary pole* $-i\delta\omega_s$ *of the matrix* $\tilde{A}$*. Later we will show in Section 6 that this imaginary pole and its associated eigenvector* (35) *are closely related to the dark state formed by the two DQD qubits.*

Finally, in the mutual resonance case, i.e., $\delta\omega_s = \delta\omega_r = 0$, the impulse response function (25) can be simplified as

$$g_{\tilde{G}}(t) = \delta(t) - \tilde{\kappa}\left(\cosh[\chi t] - \frac{\tilde{\kappa}}{4}\frac{\sinh[\chi t]}{\chi}\right) e^{-\frac{\tilde{\kappa}}{4}t}, \tag{37}$$

where $\chi = \sqrt{(\frac{\tilde{\kappa}}{4})^2 - (\Gamma_1^2 + \Gamma_2^2)}$. In particular, if $\tilde{\kappa}^2 < 16(\Gamma_1^2 + \Gamma_2^2)$, we have $\chi = i\omega_{\text{Rabi}}$, where $\omega_{\text{Rabi}} = \sqrt{\Gamma_1^2 + \Gamma_2^2 - (\frac{\tilde{\kappa}}{4})^2}$. In this case, the impulse response function (37) is

$$g_{\tilde{G}}(t) = \delta(t) - \tilde{\kappa}\left(\cos(\omega_{\text{Rabi}}t) - \frac{\tilde{\kappa}}{4}\frac{\sin(\omega_{\text{Rabi}}t)}{\omega_{\text{Rabi}}}\right) e^{-\frac{\tilde{\kappa}}{4}t}. \tag{38}$$

In the discussions of Fig. 7 in Section 5, we will show that ω_{Rabi} in (38) is actually the oscillation frequency of the two DQD qubits.

4. The steady-state output field state

4.1. The steady-state output field state

In this section, assuming the coupled system G is initialized in the state $|g_1\rangle \otimes |g_2\rangle \otimes |0\rangle$ and the input field b_0 is in a single-photon state, we aim to derive an analytic expression of the steady-state output field state in the output channel b_3.

With the aid of Lemma 3.1, we are ready to prove the main result of this section.

Theorem 4.1. *Let the quantum coherent feedback network be driven by a single-photon input state* (10)*, and the coupled system G be initialized in the state $|g_1\rangle \otimes |g_2\rangle \otimes |0\rangle$. Then the steady-state ($t_0 \to -\infty$ and $t \to \infty$) output field state of this quantum coherent feedback network is a single-photon state with the pulse shape*

$$\eta[i\omega] = \tilde{G}[i\omega]\xi[i\omega], \tag{39}$$

where the transfer function $\tilde{G}$ is given by (26)*.*

Proof. The proof follows the techniques first developed in [16, Theorem 5] for linear quantum systems and further generalized in [17, Theorem 5] to quantum finite-level systems. The result holds if the following critical conditions hold

C1. $\tilde{C}e^{\tilde{A}(t-t_0)} \langle\Phi| X(t_0) \to 0$ as $t_0 \to -\infty$;

C2. The transfer function $\tilde{G}[s]$ has no roots on the imaginary axis.

Clearly, if the matrix $\tilde{A}$ is Hurwitz stable, then both **C1** and **C2** are naturally satisfied. Hence, by Lemma 3.1, it suffices to check the marginal stability case of $\delta\omega_1 = \delta\omega_2$. Let $\delta\omega_1 = \delta\omega_2 = \delta\omega_s$ for some $\delta\omega_s \in \mathbb{R}$, then the system matrix $\tilde{A}$ can be factorized as (32). We denote $V = \{v_{ij}\}$ and $V^{-1} = \{w_{ij}\}$ with $i, j = 1, 2, 3$. It can be directly calculated that $v_{13} = 0$, $v_{23} = 1$, $v_{33} = 1$, and $w_{31} = 0$. Consequently, we have

$$\tilde{C}e^{\tilde{A}(t-t_0)} \langle\Phi| X(t_0) = \tilde{C}V^{-1}e^{\Lambda_s(t-t_0)}V \langle\Phi| X(t_0) \to 0, \tag{40}$$

as $t_0 \to -\infty$. Thus, Condition **C1** holds. Moreover, in the marginal stability case the transfer function $\tilde{G}[s]$ is reduced to be (36), in which λ_2, λ_3 are both in the L.H.S. of the complex plane. Thus, the roots of $\tilde{G}[s]$ in (36) are in the L.H.S. of the complex plane and Condition **C2** holds. Consequently, employing the techniques developed in [16, 17] one can show that the steady-state output field state is a single-photon state with pulse shape given in (39).

We end this subsection with a final remark.

Remark 4.1. *From the proof of Lemma 3.1, it is easy to see that Lemma 3.1 does not depend on the specific value of $\tilde{\kappa}$; hence it also holds for the matrix A. As a result, Theorem 4.1 also holds for the coupled system G.*

4.2. Simulations for the pulse shape of the single-photon output state

In this subsection, we illustrate Theorem 4.1 by driving the coherent feedback network with a single photon of the rising exponential pulse shape

$$\xi(t) = \begin{cases} \sqrt{\gamma}e^{\left(\frac{\gamma}{2}+i\omega_p\right)t}, & t \le 0, \\ 0, & t > 0, \end{cases} \tag{41}$$

where ω_p is the carrier frequency of the input light field. It can be shown that in the frequency domain this pulse shape has the Lorentzian spectrum and γ is the full width at half maximum (FWHM), [55]. In what follows, both the open-loop case (namely the coupled system G) and the closed-loop case (namely the coherent feedback network $\tilde{G}$) are simulated.

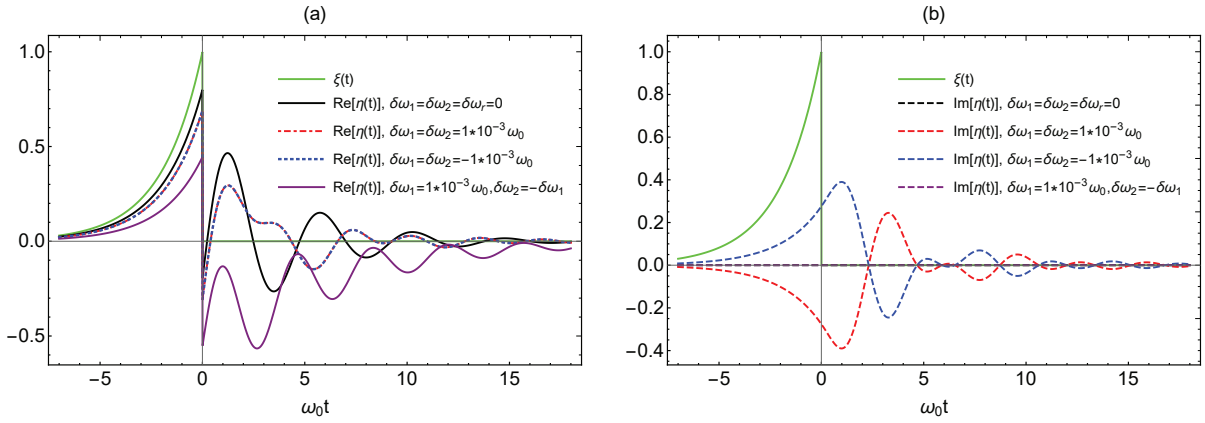

Figure 2: The green curve is the pulse shape of the single-photon input state $\xi(t)$. The black solid curve in Fig. 2(a) is the real part of the output pulse shape when the three components (two DQD qubits and the microwave cavity) are tuned into mutual resonance $\delta\omega_1 = \delta\omega_2 = \delta\omega_r = 0$, the corresponding imaginary part is presented in Fig. 2(b) by the black dashed curve. Similar descriptions are applied to the other three cases: red detuning ($\delta\omega_1 = \delta\omega_2 = 1 \times 10^{-3}\omega_0$), blue detuning ($\delta\omega_1 = \delta\omega_2 = -1 \times 10^{-3}\omega_0$), and red+blue detunings ($\delta\omega_1 = 1 \times 10^{-3}\omega_0$, $\delta\omega_2 = -1 \times 10^{-3}\omega_0$). The two DQD qubits are equally coupled to the cavity ($\Gamma_1 = \Gamma_2 = 1 \times 10^{-3}\omega_0$). The other parameters are $\kappa = \gamma = 1 \times 10^{-3}\omega_0$.

First, we look at the open-loop case, namely the system G. The simulation results are shown in Fig. 2, where it is assumed $\delta\omega_r = 0$ in all scenarios. We have the following observations.

- Firstly, it can be observed that the real parts of the output pulse shapes monotonically increase when $t \leq 0$. When $t > 0$, they start to oscillate and eventually settle to 0; see Fig. 2(a). Recall that the pulse shape of a single-photon state is the probability amplitude of the single-photon state, which gives the probability of finding the photon. Hence, the oscillating nature of the output pulse shape $\eta(t)$ implies that the photon is absorbed and emitted by the two DQD qubits from time to time, thus indicating the quantum Rabi oscillations of the DQD qubits. (This is indeed confirmed by the simulations in Section 5.) Moreover, interestingly, ω_{Rabi} in (38) is the oscillation frequency of the black solid curve in Fig. 2(a). Rabi oscillations often appear in the Jaynes-Cummings model (interaction between an atom and a resonator), where the atom alternately emits a photon into the resonator and reabsorbs it.

- Secondly, the pulse shape of the output single photon for the red detuning case and that for the blue detuning case have the same real parts (see the coincidence between the red dot-dashed curve and the blue dotted curve in Fig. 2(a)); whereas their corresponding imaginary parts are axisymmetric (see the red and blue dashed curves in Fig. 2(b)). These observations are confirmed by the following theoretical analysis. In these two cases, let $\delta\omega_1 = \delta\omega_2 = \delta\omega_s$. Let $G_+[s]$, $G_-[s]$ denote the transfer functions and $\eta_+(t)$, $\eta_-(t)$ the corresponding output pulse shapes of the red and blue detuning cases,

respectively. By (36), we have

$$G_{\pm}[i\omega] = \frac{\Gamma_1^2 + \Gamma_2^2 + (i\omega \pm i\delta\omega_s)(i\omega - \frac{\kappa}{2})}{\Gamma_1^2 + \Gamma_2^2 + (i\omega \pm i\delta\omega_s)(i\omega + \frac{\kappa}{2})}.$$

The output pulse shapes for the red(blue) detuning case are given by

$$\eta_{+(-)}(t) = \frac{1}{\sqrt{2\pi}} \int_{-\infty}^{\infty} e^{i\omega t} G_{+(-)}[i\omega]\xi[i\omega]\ d\omega,$$

respectively. Noticing

$$G_-[-i\omega] = \frac{1}{G_+[i\omega]} = G_+[i\omega]^*,$$

we have

$$\begin{aligned}
\eta_-(t) &= \frac{1}{\sqrt{2\pi}} \int_{-\infty}^{\infty} e^{-i\omega t} G_-[-i\omega]\xi[-i\omega]\ d\omega \\
&= \frac{1}{\sqrt{2\pi}} \int_{-\infty}^{\infty} e^{-i\omega t} G_+[i\omega]^*\xi[-i\omega]\ d\omega \\
&= \left(\frac{1}{\sqrt{2\pi}} \int_{-\infty}^{\infty} e^{i\omega t} G_+[i\omega]\xi[i\omega]\ d\omega \right)^* \\
&= \eta_+(t)^*.
\end{aligned}$$

In other words, the real parts of the output pulse shapes for the two cases are the same, while their imaginary parts are axisymmetric.

- Thirdly, when the three components are tuned into mutual resonance ($\delta\omega_1 = \delta\omega_2 = \delta\omega_r = 0$), the imaginary part of the output pulse shape remains 0 all the time (the black dashed curve in Fig. 2(b)). This result also holds when the detunings for these two DQD qubits are with the opposite signs (the purple dashed curve in Fig. 2(b)). Hence, phase shift can be eliminated in these two scenarios. These phenomena can be verified theoretically. Here we only demonstrate the mutual resonance case. Since the input pulse shape $\xi(t)$ in (41) is purely real in the rotating frame, it suffices to prove that the impulse response function $g_G(t)$ is a real-valued function. In the mutual resonance case, $g_G(t)$ can be calculated to be (37) by replacing $\tilde{\kappa}$ with κ. Clearly, no matter whether χ is real or purely imaginary, $g_G(t)$ is always a real-valued function. Therefore, in the case of mutual resonance, the imaginary part of the output pulse shape is 0 all the time. The case of red+blue detunings can be easily verified.

- Finally, compared with the cases of mutual resonance, red detuning and blue detuning, the oscillation of the output single photon is more obvious for the case of red+blue detunings (the purple solid curve in Fig. 2(a)), which means that the incident photon escapes from the coupled system much more slowly than for the other three cases. Since the incident photon escapes from the coupled system much slowly, it results in a relatively higher excitation probability for DQD qubits, which will be shown in Fig. 6 of Section 5.

Next, we look at the closed-loop case. Choose the beamsplitter reflection parameter $\mu = 0.6$. The other parameters are the same as those for Fig. 2. The simulation results are shown in Fig. 3. It can be seen that in contrast to the open-loop case, the oscillations of both real and imaginary parts of the output pulse shapes in all cases persist for a much longer time; in other words, coherent feedback elongates the interaction between the system and the input single photon.

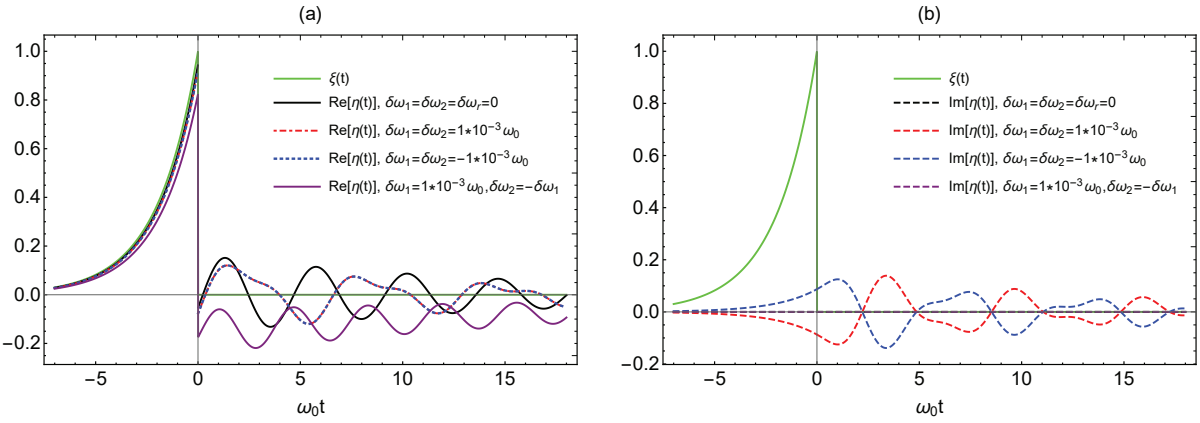

Figure 3: The single-photon input pulse shape $\xi(t)$ is plotted with the green curve, while the real and imaginary parts of the output single-photon pulse shapes for the cases of mutual resonance, red detuning, blue detuning and red+blue detunings are shown as black, red, blue and purple curves in Fig. 3(a) and (b), respectively. The two DQD qubits are equally coupled to the cavity ($\Gamma_1 = \Gamma_2 = 1 \times 10^{-3}\omega_0$). The other parameters are $\kappa = \gamma = 1 \times 10^{-3}\omega_0$, $\delta\omega_r = 0$, and $\mu = 0.6$.

5. The excitation probabilities

In Section 4, we studied how the coherent feedback network in Fig. 1 responds to a continuous-mode single-photon input state. In this section, we investigate a closely related problem: how are the DQD qubits excited by an input single photon? In particular, we compute the excitation probabilities of the first DQD qubit, thus it is named the "target DQD qubit" in this section.

Recall that $|\Phi_1\rangle$ is a single-photon state and $|\Phi_0\rangle$ is the vacuum state of the input field. Denote the expectations

$$\omega_t^{mn}(X) = \langle \eta\Phi_m | j_t(X) | \eta\Phi_n \rangle, \quad m, n = 0, 1, \tag{42}$$

where $|\eta\rangle$ is the initial state of the coupled system G, and by (6)

$$dj_t(X) = j_t(\mathcal{L}_{\text{total}}X)dt + dB^\dagger(t)j_t([X, L_{\text{total}}]) + j_t([L_{\text{total}}^\dagger, X])dB(t) \tag{43}$$

with

$$\mathcal{L}_{\text{total}}X = -i[X, H_{\text{total}}] + L_{\text{total}}^\dagger X L_{\text{total}} - \frac{1}{2}L_{\text{total}}^\dagger L_{\text{total}}X - \frac{1}{2}XL_{\text{total}}^\dagger L_{\text{total}}.$$

Define matrices $\rho^{mn}(t)$ by means of

$$\text{Tr}[\rho^{mn}(t)^\dagger X] \triangleq \omega_t^{mn}(X), \quad m, n = 0, 1. \tag{44}$$

The following result presents the master equations for the quantum coherent feedback network driven by the single-photon state $|\Phi_1\rangle$ in the Schrödinger picture.

Lemma 5.1. *[22] The Master equation for the quantum coherent feedback network driven by the single-photon state $|\Phi_1\rangle$ in (8) in the Schrödinger picture is given by a system of ordinary differential equations*

$$\begin{aligned}
\dot{\rho}^{11}(t) =& \mathcal{L}_{\text{total}}^\star \rho^{11}(t) + \xi(t)[\rho^{01}(t), L_{\text{total}}^\dagger] + \xi^*(t)[L_{\text{total}}, \rho^{10}(t)],\\
\dot{\rho}^{10}(t) =& \mathcal{L}_{\text{total}}^\star \rho^{10}(t) + \xi(t)[\rho^{00}(t), L_{\text{total}}^\dagger],\\
\dot{\rho}^{01}(t) =& \mathcal{L}_{\text{total}}^\star \rho^{01}(t) + \xi^*(t)[L_{\text{total}}, \rho^{00}(t)],\\
\dot{\rho}^{00}(t) =& \mathcal{L}_{\text{total}}^\star \rho^{00}(t),
\end{aligned} \tag{45}$$

where the initial conditions are

$$\rho^{11}(0) = \rho^{00}(0) = |\eta\rangle\langle\eta|, \quad \rho^{10}(0) = \rho^{01}(0) = 0, \tag{46}$$

with $|\eta\rangle$ *being the initial state of the coupled system* G.

In what follows, we focus on the density operator of the target DQD qubit by tracing over the cavity and the 2nd DQD qubit, the reduced density operator for the target DQD qubit is given by

$$\begin{aligned}\rho_{\mathrm{DQD}_1}(t) =& \mathrm{Tr}_{\mathrm{DQD}_2}[\mathrm{Tr}_{\mathrm{cav}}[\rho^{11}(t)]] \\ =& \langle g_2 0|\rho^{11}(t)|g_2 0\rangle + \langle g_2 1|\rho^{11}(t)|g_2 1\rangle + \langle e_2 0|\rho^{11}(t)|e_2 0\rangle + \langle e_2 1|\rho^{11}(t)|e_2 1\rangle.\end{aligned} \tag{47}$$

Let the input single-photon state $|\Phi_1\rangle$ have a Gaussian pulse shape,

$$\xi(t) = \left(\frac{\Omega^2}{2\pi}\right)^{\frac{1}{4}} \exp\left(-\frac{\Omega^2}{4}(t - t_{\mathrm{peak}})^2\right),$$

where Ω denotes the photon frequency bandwidth, and t_{peak} is the peak arrival time of the photon and fixed to be $3 * 10^{-3}\omega_0$ in the following simulations. The initial state of the coupled system G is chosen to be $|\eta\rangle = |g_1\rangle \otimes |g_2\rangle \otimes |0\rangle$. The excitation probabilities of the target DQD qubit are simulated in Figs. 4-6, where the decay rate of the cavity is $\kappa = 1.5 \times 10^{-3}\omega_0$, and the photon frequency bandwidth $\Omega = 2.75\kappa$, we choose the beamsplitter parameter $\mu = 0.2$.

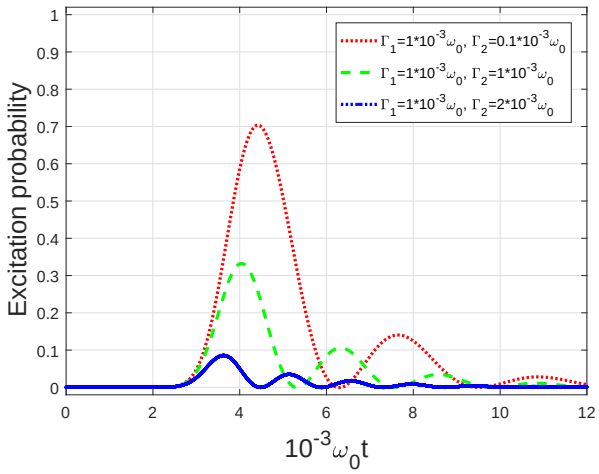

Figure 4: The excitation probability of the target DQD qubit with different couplings Γ_2. $\delta\omega_1 = \delta\omega_2 = \delta\omega_r = 0$.

In Figs. 4 and 5, we plot the excitation probability of the target DQD qubit with different couplings and detunings, respectively. It can be observed that the excitation probability of the target DQD qubit can be significantly improved by reducing the coupling Γ_2 or increasing the detuning $\delta\omega_2$ of the 2nd DQD qubit, which results in a weak interaction between the cavity and the 2nd DQD qubit.

In Fig. 6, we plot the excitation probability of the target DQD qubit for three cases: red detuning ($\delta\omega_1 = \delta\omega_2 = 1 \times 10^{-3}\omega_0$), blue detuning ($\delta\omega_1 = \delta\omega_2 = -1 \times 10^{-3}\omega_0$) and red+blue detunings ($\delta\omega_1 = 1 \times 10^{-3}\omega_0$, $\delta\omega_2 = -1 \times 10^{-3}\omega_0$). It can be observed that when the detunings for the two DQD qubits are with the same sign, the excitation probabilities of the target DQD qubit are identical. This can be

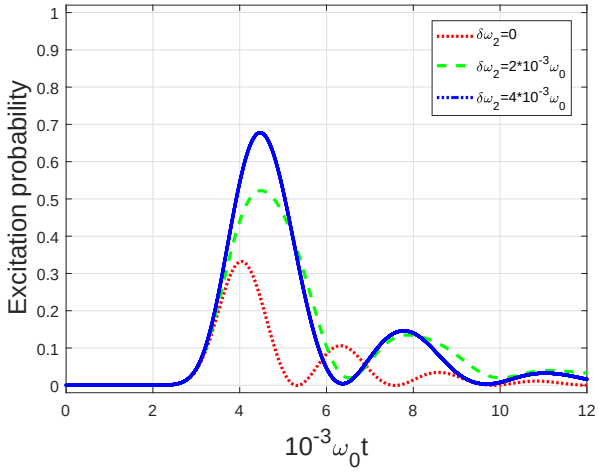

Figure 5: The excitation probability of the target DQD qubit with different detunings $\delta\omega_2$. The couplings are $\Gamma_1 = \Gamma_2 = 1 \times 10^{-3}\omega_0$. And $\delta\omega_r = 0$.

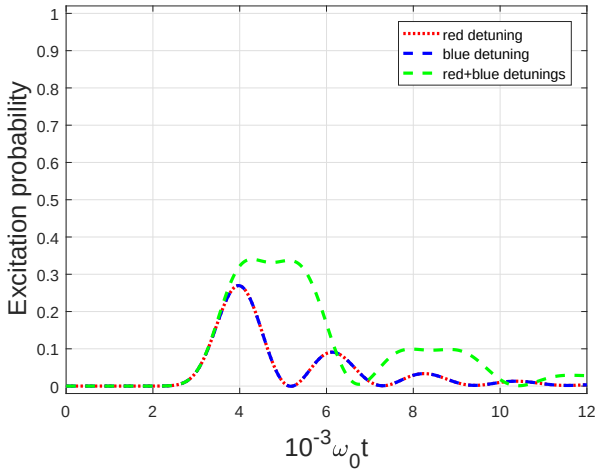

Figure 6: The excitation probability of the target DQD qubit with the cases of red detuning, blue detuning and red+blue detunings. The couplings are $\Gamma_1 = \Gamma_2 = 1 \times 10^{-3}\omega_0$. And $\delta\omega_r = 0$.

explained by the form of system Hamiltonian given in (14). Specifically, changing the signs of $\delta\omega_1$ and $\delta\omega_2$ simultaneously is equivalent to rewriting the Pauli matrix σ_z as $-\sigma_z$. By the master equations (45), the term $-\frac{i}{2}\delta\omega_k\sigma_{z,k}\rho + \frac{i}{2}\delta\omega_k\rho\sigma_{z,k}$ will be changed to $-\frac{i}{2}\delta\omega_k\rho\sigma_{z,k} + \frac{i}{2}\delta\omega_k\sigma_{z,k}\rho$, $k = 1, 2$, which has no effect on the excitation probability. On the other hand, in general, in the red+blue detuning case the excitation probability is higher than the other two cases. Moreover, even when time is relatively large, the excitation probability in the red+blue detuning case is still not close to zero, which is consistent with the output photon distribution exhibited by the purple solid curve in Fig. 2(a).

Finally, for comparison we consider the cases that the coherent feedback network is driven by the vacuum state $|\Phi_0\rangle$ instead of the single-photon state; however, one of the DQD qubits is in its excited state or there is a photon initially in the cavity. In this case, the reduced density operator for the target DQD qubit is given by

$$\begin{aligned}\rho_{\mathrm{DQD}_1}(t) =& \mathrm{Tr}_{\mathrm{DQD}_2}[\mathrm{Tr}_{\mathrm{cav}}[\rho^{00}(t)]]\\ =& \langle g_2 0|\rho^{00}(t)|g_2 0\rangle + \langle g_2 1|\rho^{00}(t)|g_2 1\rangle + \langle e_2 0|\rho^{00}(t)|e_2 0\rangle + \langle e_2 1|\rho^{00}(t)|e_2 1\rangle.\end{aligned}$$

The simulation results are shown in Fig. 7, where all three transitions are tuned into mutual resonance ($\delta\omega_1 = \delta\omega_2 = \delta\omega_r = 0$).

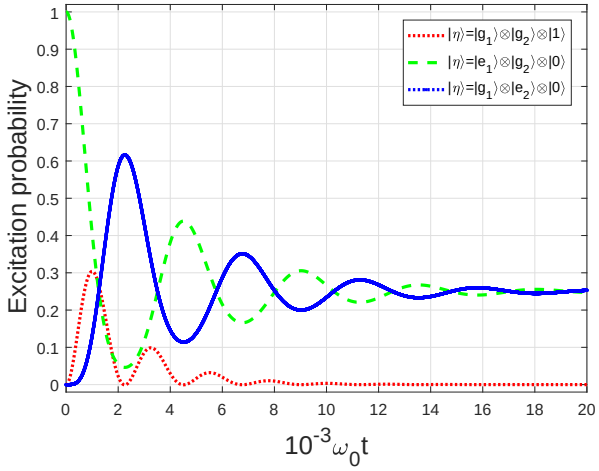

Figure 7: The excitation probability of the target DQD qubit with different initial states. We choose $\Gamma_1 = \Gamma_2 = 1 \times 10^{-3}\omega_0$, $\kappa = 1.5 \times 10^{-3}\omega_0$ and $\mu = 0.2$.

In Fig. 7, it can be observed that the excitation probability will eventually be 0 when the single photon is initially in the cavity (the red dotted curve), which indicates that the single photon escapes from the quantum coherent feedback network in the end. However, the excitation probability of the target DQD qubit approaches 0.25 when the two DQD qubits are equally coupled to the cavity and the initial state of the coupled system is $|e_1\rangle \otimes |g_2\rangle \otimes |0\rangle$ or $|g_1\rangle \otimes |e_2\rangle \otimes |0\rangle$; see the green and blue dotted curves. Although the green and blue curves have the same stationary excitation probability, the crests and troughs are exactly symmetrical during the transient dynamics. This is consistent with the experimental result given in [34, Fig. 4c], in which the coherent oscillations between the two superconducting qubits emerges symmetrically. To be more specific, the green and blue curves can be respectively regarded as the excitation probabilities of the first and second DQD qubits under the same initial state $|e_1\rangle \otimes |g_2\rangle \otimes |0\rangle$, which are demonstrated by

the measured homodyne voltages for $|\uparrow\downarrow\rangle$ and $|\downarrow\uparrow\rangle$ in [34, Fig. 4c], respectively. Moreover, $\omega_{\rm Rabi}$ in (38) can be calculated by the parameters κ, Γ_1, Γ_2 in Fig. 7. We find in Fig. 7 that the oscillation period $T \approx \frac{2\pi}{\omega_{\rm Rabi}}$, which indicates that $\omega_{\rm Rabi}$ in (38) is also the Rabi frequency of the coherent oscillation in Fig. 7. Finally, the amplitudes of vibration are getting smaller and smaller due to the decay of the cavity.

Remark 5.1. *It is noteworthy to mention that the discussions above are based on the assumption that all three transitions are tuned into mutual resonance $\delta\omega_1 = \delta\omega_2 = \delta\omega_r = 0$. In the next section, we show that when the two DQD qubits are both equally red- (blue-) detuned ($\delta\omega_1 = \delta\omega_2 \neq 0$, $\delta\omega_r = 0$), the excitation probability of the target DQD qubit eventually settles to the same value as that for the mutual resonance case. However, when the two DQD qubits are with red+blue detunings ($\delta\omega_1 = -\delta\omega_2 \neq 0$, $\delta\omega_r = 0$), the excitation probability is eventually 0, which means that the single photon eventually escapes from the quantum coherent feedback network.*

6. An analytic result

The simulation results in Fig. 7 indicate that, when the quantum coherent feedback is driven by a vacuum state while one of the DQD qubits is initially in the excited state, the excitation probability of the target DQD qubit eventually settles to a non-zero value. In this section, we present an analytic result to explain these simulations.

The main result of this section is the following theorem.

Theorem 6.1. *Assume that the first DQD qubit is initialized in the excited state, the second DQD qubit is initialized in the ground state, the cavity is initially empty and the quantum coherent feedback network is driven by the vacuum input state, i.e., the initial joint system-field state is $|e_1g_20\Phi_0\rangle$. If the transition frequencies of the two DQD qubits are not equal ($\delta\omega_1 \neq \delta\omega_2$), then the steady state of the two DQD qubits is a pure state $|\Phi_{\rm DQD}(\infty)\rangle = |g_1g_2\rangle$. Otherwise, when $\delta\omega_1 = \delta\omega_2 = \delta\omega_s$ for some $\delta\omega_s \in \mathbb{R}$, the steady-state joint system-field state is*

$$|\Psi(\infty)\rangle = s_1(\infty)\,|g_1g_20\Phi_1\rangle + s_2(\infty)|g_1e_20\Phi_0\rangle + s_3(\infty)|e_1g_20\Phi_0\rangle, \tag{48}$$

where

$$|s_1(\infty)|^2 = \frac{\Gamma_1^2}{\Gamma_1^2+\Gamma_2^2}, \quad s_2(\infty) = -\frac{\Gamma_1\Gamma_2}{\Gamma_1^2+\Gamma_2^2}, \quad s_3(\infty) = \frac{\Gamma_2^2}{\Gamma_1^2+\Gamma_2^2}, \tag{49}$$

and $|\Phi_1\rangle$ is a single-photon state in the output field with the pulse shape

$$\eta(t) = \frac{\Gamma_1\sqrt{\tilde{\kappa}}\sinh(\lambda' t)}{i\lambda' s_1(0)} e^{-\frac{1}{4}[\tilde{\kappa}+2i(\delta\omega_r+\delta\omega_s)]t}, \tag{50}$$

where $|s_1(0)|^2 = \frac{\Gamma_1^2}{\Gamma_1^2+\Gamma_2^2}$, and λ' is given by (34).

proof As there is only one excitation, the joint system-field state $|\Psi(t)\rangle$ is of the form

$$|\Psi(t)\rangle = s_1(t)\int_0^t \eta(\tau)b^\dagger(\tau)d\tau|g_1g_20\Phi_0\rangle + s_2(t)|g_1e_20\Phi_0\rangle + s_3(t)|e_1g_20\Phi_0\rangle + s_4(t)|g_1g_21\Phi_0\rangle, \tag{51}$$

where the initial condition is $s_2(0) = s_4(0) = 0$ and $s_3(0) = 1$. $\eta(\tau)$ denotes the pulse shape of the single-photon output state with $\|\eta\| = 1$. As the integral is 0 at the initial time $t = 0$, it is not necessary to impose an initial condition on $s_1(t)$. The normalization condition for $|\Psi(t)\rangle$ is

$$|s_1(t)|^2\int_0^t |\eta(\tau)|^2 d\tau + \sum_{j=2}^4 |s_j(t)|^2 = 1, \tag{52}$$

which in the stationary state ($t \to \infty$) is

$$\sum_{j=1}^{4} |s_j(\infty)|^2 = 1. \tag{53}$$

By (3)-(4) and [45, Eq. (11.2.18)], we have the following Itō QSSE

$$\begin{aligned} d\,|\Psi(t)\rangle =& \left\{ -\left(\frac{1}{2}L_{\rm sys}^{\dagger}L_{\rm sys} + iH_{\rm sys}\right)dt + LdB^{\dagger}(t)\right\}|\Psi(t)\rangle \\ =& \left\{\left[-i\delta\omega_r + \frac{i}{2}\delta\omega_1 + \frac{i}{2}\delta\omega_2 - \frac{\tilde{\kappa}}{2}\right]s_4(t) - i\Gamma_1 s_3(t) - i\Gamma_2 s_2(t)\right\}|g_1g_2 1\Phi_0\rangle\,dt \\ &+ \left[\frac{i}{2}(\delta\omega_1 - \delta\omega_2)s_2(t) - i\Gamma_2 s_4(t)\right]|g_1e_2 0\Phi_0\rangle\,dt \\ &- \left[\frac{i}{2}(\delta\omega_1 - \delta\omega_2)s_3(t) + i\Gamma_1 s_4(t)\right]|e_1g_2 0\Phi_0\rangle\,dt \\ &+ \left[\frac{i}{2}(\delta\omega_1 + \delta\omega_2)s_1(t)\int_0^t \eta(\tau)b^{\dagger}(\tau)d\tau\right]|g_1g_2 0\Phi_0\rangle\,dt \\ &+ \sqrt{\tilde{\kappa}}s_4(t)dB^{\dagger}(t)\,|g_1g_2 0\Phi_0\rangle\,. \end{aligned} \tag{54}$$

On the other hand, differentiating (51) with respect to t, yields

$$\begin{aligned} d|\Psi(t)\rangle =& \dot{s}_4(t)\,|g_1g_2 1\Phi_0\rangle\,dt + \dot{s}_2(t)\,|g_1e_2 0\Phi_0\rangle\,dt + \dot{s}_3(t)\,|e_1g_2 0\Phi_0\rangle\,dt \\ &+ s_1(t)\eta(t)dB^{\dagger}(t)\,|g_1g_2 0\Phi_0\rangle + \left[\dot{s}_1(t)\int_0^t \eta(\tau)b^{\dagger}(\tau)d\tau\right]|g_1g_2 0\Phi_0\rangle\,dt. \end{aligned} \tag{55}$$

By comparing the first 3 terms in (54) and (55), one can get that

$$\begin{cases} \dot{s}_2(t) = \dfrac{i}{2}(\delta\omega_1 - \delta\omega_2)s_2(t) - i\Gamma_2 s_4(t), \\ \dot{s}_3(t) = -\dfrac{i}{2}(\delta\omega_1 - \delta\omega_2)s_3(t) - i\Gamma_1 s_4(t), \\ \dot{s}_4(t) = \left[-i\delta\omega_r + \dfrac{i}{2}\delta\omega_1 + \dfrac{i}{2}\delta\omega_2 - \dfrac{\tilde{\kappa}}{2}\right]s_4(t) - i\Gamma_1 s_3(t) - i\Gamma_2 s_2(t), \end{cases} \tag{56}$$

with the initial condition $[s_2(0)\ \ s_3(0)\ \ s_4(0)] = [0\ \ 1\ \ 0]$. In what follows, we find the stationary solution of (56) by sending $t \to \infty$.

If $\delta\omega_1 \neq \delta\omega_2$, it can be readily shown that the stationary solution of (56) is

$$s_2(\infty) = s_3(\infty) = s_4(\infty) = 0. \tag{57}$$

Moreover, by (53), $s_1(\infty) = 1$. Thus, in this case the steady-state joint system-field state is

$$|\Psi(\infty)\rangle = \int_0^{\infty} \eta(\tau)b^{\dagger}(\tau)d\tau|g_1g_2 0\Phi_0\rangle = |g_1g_2 0\Phi_1\rangle\,, \tag{58}$$

where $|\Phi_1\rangle \triangleq \int_0^{\infty} \eta(\tau)b^{\dagger}(\tau)d\tau\,|\Phi_0\rangle$ is a single-photon state. In other words, eventually the two DQD qubits are in the ground state, the cavity is empty, and the output field contains a single photon.

If $\delta\omega_1 = \delta\omega_2 = \delta\omega_s$, solving (56) under the initial condition $[s_2(0) \;\; s_3(0) \;\; s_4(0)] = [0 \;\; 1 \;\; 0]$, we get

$$\begin{aligned} s_2(t) &= -\frac{\Gamma_1\Gamma_2}{\Gamma_1^2+\Gamma_2^2} + \frac{\Gamma_1\Gamma_2}{2}\left(\frac{e^{\lambda_1' t}}{\lambda_1'\lambda'} - \frac{e^{\lambda_2' t}}{\lambda_2'\lambda'}\right), \\ s_3(t) &= \frac{\Gamma_2^2}{\Gamma_1^2+\Gamma_2^2} + \frac{\Gamma_1^2(\lambda_2' e^{\lambda_1' t} - \lambda_1' e^{\lambda_2' t})}{2\lambda_1'\lambda_2'\lambda'}, \\ s_4(t) &= \frac{i\Gamma_1(e^{\lambda_1' t} - e^{\lambda_2' t})}{2\lambda'}, \end{aligned} \tag{59}$$

where

$$\begin{aligned} \lambda_1' &= -\frac{1}{4}\left[\tilde{\kappa} + 2i(\delta\omega_r - \delta\omega_s)\right] - \lambda', \\ \lambda_2' &= -\frac{1}{4}\left[\tilde{\kappa} + 2i(\delta\omega_r - \delta\omega_s)\right] + \lambda', \end{aligned} \tag{60}$$

and λ' is given by (34). Sending $t \to \infty$, (59) becomes

$$s_2(\infty) = -\frac{\Gamma_1\Gamma_2}{\Gamma_1^2+\Gamma_2^2}, \quad s_3(\infty) = \frac{\Gamma_2^2}{\Gamma_1^2+\Gamma_2^2}, \quad s_4(\infty) = 0. \tag{61}$$

Moreover, by comparing the last two terms in (54) and (55), we get

$$\dot{s}_1(t) = i\delta\omega_s s_1(t), \quad s_1(t)\eta(t) = \sqrt{\tilde{\kappa}} s_4(t), \tag{62}$$

which yield

$$s_1(t) = e^{i\delta\omega_s t} s_1(0), \quad \eta(t) = \sqrt{\tilde{\kappa}}\frac{s_4(t)}{s_1(t)}. \tag{63}$$

By (63) and the normalization condition (53), we have $|s_1(\infty)|^2 = |s_1(0)|^2 = \frac{\Gamma_1^2}{\Gamma_1^2+\Gamma_2^2}$. Furthermore, inserting (59) into (63), the pulse shape of the single-photon state in the output field can be calculated as

$$\eta(t) = \frac{\Gamma_1\sqrt{\tilde{\kappa}}\sinh(\lambda' t)}{i\lambda' s_1(0)} e^{-\frac{1}{4}[\tilde{\kappa} + 2i(\delta\omega_r + \delta\omega_s)]t}, \tag{64}$$

where λ' is given by (34). In summary, in this case the steady-state joint system-field state is that given by (48).

Remark 6.1. *In Theorem 6.1, $s_1(0)$ in (50) can be written as $s_1(0) = \frac{\Gamma_1 e^{i\vartheta}}{\sqrt{\Gamma_1^2+\Gamma_2^2}}$, where ϑ is an arbitrary phase parameter. Then the pulse shape of the single-photon state (64) is*

$$\eta(t) = \frac{-ie^{-i\vartheta}\sqrt{\tilde{\kappa}(\Gamma_1^2+\Gamma_2^2)}\sinh(\lambda' t)}{\lambda'} e^{-\frac{1}{4}[\tilde{\kappa} + 2i(\delta\omega_r + \delta\omega_s)]t}. \tag{65}$$

Thus, the output single photon cannot distinguish the two DQD qubits.

Remark 6.2. *Consider the mutual resonant case ($\omega_1 = \omega_2 = \omega_r$) and let the decay rate $\kappa = 0$. Then the single photon initially in the first DQD can bounce among the two DQDs and the cavity. Assume further the two DQD qubits are equally coupled to the cavity, in other words, $\Gamma_1 = \Gamma_2 = \Gamma$. According to (34) and (60),*

$$\lambda' = i\sqrt{2}\Gamma, \quad \lambda_1' = -\lambda', \quad \lambda_2' = \lambda'. \tag{66}$$

In this case, the amplitudes (59) *of the states* $|g_1e_20\Phi_0\rangle$, $|e_1g_20\Phi_0\rangle$ *and* $|g_1g_21\Phi_0\rangle$ *are reduced to be*

$$\begin{aligned} s_2(t) &= -\frac{1}{2} + \frac{1}{2}\cos\left(\sqrt{2}\Gamma t\right), \\ s_3(t) &= \frac{1}{2} + \frac{1}{2}\cos\left(\sqrt{2}\Gamma t\right), \\ s_4(t) &= \frac{1}{i\sqrt{2}}\sin\left(\sqrt{2}\Gamma t\right). \end{aligned} \tag{67}$$

By (67)*, the photon is transferred among the three states with the coherent oscillation period* $T = \frac{2\pi}{\sqrt{2}\Gamma}$ *[33]. A quarter period* $\frac{1}{4}T = \frac{\pi}{2\sqrt{2}\Gamma}$ *corresponds to a universal* $\sqrt{i\text{SWAP}}$ *gate, which entangles the two DQD qubits [62, 34]. In fact, in this case the joint system-field state is*

$$\left(\frac{1}{i\sqrt{2}}|g_1g_2\rangle \otimes |1\rangle + \frac{1}{2}(|e_1g_2\rangle - |g_1e_2\rangle) \otimes |0\rangle\right) \otimes |\Phi_0\rangle, \tag{68}$$

which shows evidently that the two qubits are entangled. On the other hand, a half period $\frac{1}{2}T = \frac{\pi}{\sqrt{2}\Gamma}$*, which is often referred to as a full vacuum-Rabi period, corresponds to an* iSWAP *gate, which swaps the states of the two DQD qubits, as evidenced by* $s_2\left(t + \frac{T}{2}\right) = -s_3(t)$ *and* $s_3\left(t + \frac{T}{2}\right) = -s_2(t)$*.*

Remark 6.3. *When the two DQD qubits have the same transition frequency* ($\omega_1 = \omega_2$)*, by Theorem 6.1 we see that in the steady state the output field and the two DQD qubits are in a superposition pure state* (48)*, which means that a photon exists simultaneously in the output free-propagating field and inside the 2-DQD qubit system. If* $\Gamma_1 = 0$*, i.e., the first DQD qubit is decoupled from the other components. In this case, the whole system is in the state* $|e_1g_20\Phi_0\rangle$*. This is confirmed by* (48)*. On the other hand, if* $\Gamma_2 = 0$*, then the second DQD qubit is decoupled. In this case,* (48) *reduces to* $|g_1g_20\Phi_1\rangle$*; in other words, the output field contains a single photon, while both DQD qubits are left in their ground state and the cavity is empty.*

Remark 6.4. *Comparing the expression* (48) *with the bright states* $|\pm\rangle_{r3}$ *for the coherent input case in [38, Fig. 2], each DQD qubit being in its excited state shares the same ratio of probability* Γ_1^2/Γ_2^2*. However, in contrast to the fixed probability* $1/2$ *in [38, Fig. 2], the probability of the two coupled DQD qubits in the ground state* $|g_1g_2\rangle$ *is controllable with the value* $\frac{\Gamma_1^2}{\Gamma_1^2+\Gamma_2^2}$*, which is also the probability of the single-photon escaping from the coupled system. By Theorem 6.1, it can be seen that the steady state of the whole system is independent of the cavity decay rate* κ *and beamsplitter parameter* μ*.*

Remark 6.5. *The 2nd and 3rd terms of* (48) *can be rewritten as*

$$\frac{\Gamma_2}{\Gamma_1^2+\Gamma_2^2}\Big[(\Gamma_2|e_1g_2\rangle - \Gamma_1|g_1e_2\rangle) \otimes |0\rangle + 0\,|g_1g_2\rangle \otimes |1\rangle\Big] \otimes |\Phi_0\rangle. \tag{69}$$

It is interesting to observe that the amplitudes inside the square bracket $(\Gamma_2, -\Gamma_1, 0)$ *are exactly the coefficients of* (35) *for the eigenstate associated with the imaginary pole* $-i\delta\omega_s$*. The state* (69) *is of the form of dark state* $|2, 1d\rangle$ *given in [35]. Consequently, the steady state* (48) *of the joint system-field given in Theorem 6.1 is a superposition of a free propagating photon and a dark state of the DQD-DQD system.*

We end this section with the following result, which is a consequence of Theorems 4.1 and 6.1.

Corollary 6.1. *Let the two DQD qubits be initialized in the ground state and the cavity is initially empty. Neither of these two DQD qubits can be fully excited by a single photon of an arbitrary pulse shape.*

Proof. We prove this result by contradiction. Suppose that an input single photon of a certain pulse shape is able to fully excite the first DQD qubit at time t_0. Then at this time instant, the joint system-field state is $|\Psi(t_0)\rangle = |e_1 g_2 0 \Phi_0\rangle$. By Theorem 6.1, the steady-state joint system-field state is of the form (48); in other words, it is a superposition of the single-photon output state and the dark state of the DQD-DQD qubits. However, by Theorem 4.1, if the two DQD qubits are initialized in the ground state, the cavity is initially empty, and the system is driven by a single-photon input state, then the steady-state output field is a single-photon state and the system is eventually in the state $|g_1 g_2 0\rangle$. We have reached a contradiction.

Remark 6.6. *In [63, Theorem 1], it is shown that a two-level system inside a cavity can be fully excited by an input single photon of a particular pulse shape. Corollary 6.1 above tells us this is not the case if there are* two *two-level systems coupled to a cavity. The reason is simple: the single two-level system itself in the cavity cannot have a dark state, thus eventually it settles in the ground state and the output field contains a single free-propagating photon.*

7. Conclusion

In this paper, we have studied in detail the dynamics of a quantum coherent feedback network of two distant DQD qubits which are directly coupled to a cavity. The main results of this paper is summarized below.

Firstly, when the two DQD qubits are initialized in the ground state and the cavity is empty, an analytic expression of the output single-photon state has been derived when the system is driven by a continuous-mode single-photon state. To establish this result, the Routh like table and the Sign Pair Criterion (SPC) recently developed in [58] are utilized. Moreover, techniques for single photon processing developed in [16, 17] are also employed. Theorem 4.1 has been illustrated by using a single photon of an exponentially rising pulse shape to drive the coherent feedback network. Differences among mutual resonant, red detuned, blue detuned, and red+blue detuned dynamics have been demonstrated. Moreover, it has been observed that coherent feedback elongates considerably the interaction between the input single photon and the system. Generally speaking, as there is only one excitation in this system, the essential system dynamics are well captured by a transfer function. Indeed, properties such as oscillation frequency and axisymmetry of the simulation curves can be explained by a transfer function and its corresponding impulse response function.

Secondly, the excitation of the DQD qubits driven by a single-photon input state has been investigated. In particular, it has been indicated that red+blue detunings allow higher excitation probabilities. Moreover, the interaction time between the photon and the two DQD qubits is much longer in the red+blue detuning case in contrast to the other cases. Particularly, when one of the two DQD qubits is initialized in its excited state while the coherent feedback network is driven by a vacuum input, interesting system dynamics are observed in Fig. 7.

Finally, assuming that one DQD qubit is initialized in its excited state while the system is driven by a vacuum input, an explicit form of the steady-state joint system-field state has been derived by means of the quantum stochastic Schrödinger equation (QSSE). In particular, it has been shown that the joint system-field state is an entangled state composed of a single-photon state of the output free-propagating field and a dark state of the two DQD qubits when the transition frequencies of the two DQD qubits are equal to each other.

Acknowledgement

This research is partially supported by Hong Kong Research Grant Council under Grants Nos. 15203619 and 15208418, Shenzhen Fundamental Research Fund, China, under Grant No. JCYJ20190813165207290, National Natural Science Foundation of China under Grants Nos. 62003111, 62173288, 62273154, Natural Science Foundation of Guangdong Province under Grant No. 2022A1515010390, and the CAS AMSS-polyU Joint Laboratory of Applied Mathematics.

References

[1] N. Gisin, R. Thew, Quantum communication, Nature Photonics 1 (3) (2007) 165–171.

[2] H. J. Kimble, The quantum internet, Nature 453 (7198) (2008) 1023–30.

[3] L. Bouten, R. V. Handel, M. R. James, An introduction to quantum filtering, SIAM Journal on Control and Optimization 46 (6) (2007) 21992241.

[4] C. Wu, B. Qi, C. Chen, D. Dong, Robust learning control design for quantum unitary transformations, IEEE Transactions on Cybernetics 47 (12) (2017) 4405–4417.

[5] J. Braumüller, M. Marthaler, A. Schneider, A. Stehli, H. Rotzinger, M. Weides, A. V. Ustinov, Analog quantum simulation of the rabi model in the ultra-strong coupling regime, Nature communications 8 (1) (2017) 779.

[6] D. Lv, S. An, Z. Liu, J.-N. Zhang, J. S. Pedernales, L. Lamata, E. Solano, K. Kim, Quantum simulation of the quantum rabi model in a trapped ion, Physical Review X 8 (2018) 021027.

[7] P. Forn-Díaz, L. Lamata, E. Rico, J. Kono, E. Solano, Ultrastrong coupling regimes of light-matter interaction, Reviews of Modern Physics 91 (2) (2019) 025005.

[8] S. Cong, M. Gao, G. Cao, G. Guo, G. Guo, Ultrafast manipulation of a double quantum-dot charge qubit using lyapunov-based control method, IEEE Journal of Quantum Electronics 51 (8) (2015) 1–8.

[9] W. Cui, D. Dong, Modeling and control of quantum measurement-induced backaction in double quantum dots, IEEE Transactions on Control Systems Technology (2018).

[10] D. E. Chang, A. S. Sørensen, E. A. Demler, M. D. Lukin, A single-photon transistor using nanoscale surface plasmons, Nature Physics 3 (11) (2007) 807.

[11] L. Neumeier, M. Leib, M. J. Hartmann, Single-photon transistor in circuit quantum electrodynamics, Physical Review Letters 111 (6) (2013) 063601.

[12] W. Chen, K. M. Beck, R. Bücker, M. Gullans, M. D. Lukin, H. Tanji-Suzuki, V. Vuletić, All-optical switch and transistor gated by one stored photon, Science 341 (6147) (2013) 768–770.

[13] J. T. Shen, S. Fan, Coherent photon transport from spontaneous emission in one-dimensional waveguides, Optics Letters 30 (15) (2005) 2001–2003.

[14] S. Fan, S. E. Kocabas, J. T. Shen, Input-output formalism for few-photon transport in one-dimensional nanophotonic waveguides coupled to a qubit, Physical Review A 82 (2010) 063821.

[15] E. Rephaeli, S. Fan, Stimulated emission from a single excited atom in a waveguide, Physical Review Letters 108 (14) (2012) 143602.

[16] G. Zhang, M. R. James, On the response of quantum linear systems to single photon input fields, IEEE Transactions on Automatic Control 58 (5) (2013) 1221–1235.

[17] Y. Pan, G. Zhang, M. R. James, Analysis and control of quantum finite-level systems driven by single-photon input states, Automatica 69 (2016) 18 – 23.

[18] G. Zhang, Single-photon coherent feedback control and filtering, Springer London, London, 2020, pp. 1–4.

[19] G. Zhang, Z. Dong, Linear quantum systems: a tutorial, Annual Reviews in Control (54) (2012) 274–294.

[20] G. Zhang, Analysis of quantum linear systems response to multi-photon states, Automatica 50 (2) (2014) 442–451.

[21] G. Zhang, Dynamical analysis of quantum linear systems driven by multi-channel multi-photon states, Automatica 83 (2017) 186–198.

[22] J. E. Gough, M. R. James, H. I. Nurdin, J. Combes, Quantum filtering for systems driven by fields in single-photon states or superposition of coherent states, Physical Review A 86 (4) (2012) 043819.

[23] A. R. R. Carvalho, M. R. Hush, M. R. James, Cavity driven by a single photon: Conditional dynamics and nonlinear phase shift, Physical Review A 86 (2) (2012) 023806.

[24] G. Zhang, M. R. James, Quantum feedback networks and control: a brief survey, Chinese Science Bulletin 57 (18) (2012) 2200–2214.

[25] H. Song, G. Zhang, Z. Xi, Continuous-mode multiphoton filtering, SIAM Journal on Control and Optimization 54 (3) (2016) 1602–1632.

[26] J. Zhang, Y.-X. Liu, R.-B. Wu, K. Jacobs, F. Nori, Quantum feedback: theory, experiments, and applications, Physics Reports 679 (2017) 1–60.

[27] Z. Dong, G. Zhang, N. H. Amini, Single-photon quantum filtering with multiple measurements, International Journal of Adaptive Control and Signal Processing 32 (3) (2018) 528–546.

[28] Q. Gao, G. Zhang, I. R. Petersen, An exponential quantum projection filter for open quantum systems, Automatica 99 (2019) 59–68.

[29] Q. Gao, G. Zhang, I. R. Petersen, An improved quantum projection filter, Automatica 112 (2020) 108716.

[30] M. Benito, J. R. Petta, G. Burkard, Optimized cavity-mediated dispersive two-qubit gates between spin qubits, Physical Review B 100 (8) (2019) 081412.

[31] A. Warren, E. Barnes, S. E. Economou, Long-distance entangling gates between quantum dot spins mediated by a superconducting resonator, arXiv:1902.05704 (2019).

[32] F. Borjans, X. Croot, X. Mi, M. Gullans, J. Petta, Resonant microwave-mediated interactions between distant electron spins, Nature 577 (7789) (2020) 195–198.

[33] M. A. Sillanpää, J. I. Park, R. W. Simmonds, Coherent quantum state storage and transfer between two phase qubits via a resonant cavity, Nature 449 (7161) (2007) 438–442.

[34] J. Majer, J. Chow, J. Gambetta, J. Koch, B. Johnson, J. Schreier, L. Frunzio, D. Schuster, A. A. Houck, A. Wallraff, et al., Coupling superconducting qubits via a cavity bus, Nature 449 (7161) (2007) 443–447.

[35] J. M. Fink, R. Bianchetti, M. Baur, M. Göppl, L. Steffen, S. Filipp, P. J. Leek, A. Blais, A. Wallraff, Dressed collective qubit states and the tavis-cummings model in circuit qed, Physical Review Letter 103 (2009) 083601.

[36] T. Astner, S. Nevlacsil, N. Peterschofsky, A. Angerer, S. Rotter, S. Putz, J. Schmiedmayer, J. Majer, Coherent coupling of remote spin ensembles via a cavity bus, Physical Review Letters 118 (14) (2017) 140502.

[37] G.-W. Deng, D. Wei, S.-X. Li, J. Johansson, W.-C. Kong, H.-O. Li, G. Cao, M. Xiao, G.-C. Guo, F. Nori, et al., Coupling two distant double quantum dots with a microwave resonator, Nano letters 15 (10) (2015) 6620–6625.

[38] D. J. van Woerkom, P. Scarlino, J. H. Ungerer, C. Müller, J. V. Koski, A. J. Landig, C. Reichl, W. Wegscheider, T. Ihn, K. Ensslin, et al., Microwave photon-mediated interactions between semiconductor qubits, Physical Review X 8 (4) (2018) 041018.

[39] B. Wang, T. Lin, H. Li, S. Gu, M. Chen, G. Guo, H. Jiang, X. Hu, G. Cao, G. Guo, Correlated spectrum of distant semiconductor qubits coupled by microwave photons, Science Bulletin 66 (4) (2021) 332–338.

[40] R. L. Hudson, K. R. Parthasarathy, Quantum ito's formula and stochastic evolutions, Communications in mathematical physics 93 (3) (1984) 301–323.

[41] J. E. Gough, M. R. James, The series product and its application to quantum feedforward and feedback networks, IEEE Transactions on Automatic Control 54 (11) (2009) 2530–2544.

[42] N. Tezak, A. Niederberger, D. S. Pavlichin, G. Sarma, H. Mabuchi, Specification of photonic circuits using quantum hardware description language, Philosophical Transactions of the Royal Society A: Mathematical, Physical and Engineering Sciences 370 (1979) (2012) 5270–5290.

[43] J. Combes, J. Kerckhoff, M. Sarovar, The SLH framework for modeling quantum input-output networks, Advances in Physics: X 2 (3) (2017) 784–888.

[44] M. R. James, Quantum Networks, Springer London, London, 2020.

[45] C. Gardiner, P. Zoller, Quantum Noise: A Handbook of Markovian and Non-Markovian Quantum Stochastic Methods with Applications to Quantum Optics, Vol. 56, Springer Science & Business Media, 2004.

[46] J. E. Gough, G. Zhang, On realization theory of quantum linear systems, Automatica 59 (2015) 139–151.

[47] Y. Liu, S. Kuang, S. Cong, Lyapunov-based feedback preparation of ghz entanglement of n -qubit systems, IEEE Transactions on Cybernetics 47 (11) (2017) 3827–3839.

[48] D. F. Walls, G. J. Milburn, Quantum Optics, 2nd ed., Berlin: Springer, 2008.

[49] H. M. Wiseman, G. J. Milburn, Quantum measurement and control, Cambridge university press, 2010.

[50] D. Dong, I. R. Petersen, Quantum control theory and applications: a survey, IET Control Theory & Applications 4 (12) (2010) 2651–2671.

[51] C. Altafini, F. Ticozzi, Modeling and control of quantum systems: An introduction, IEEE Transactions on Automatic Control 57 (8) (2012) 1898–1917.

[52] M. Mirrahimi, P. Rouchon, Dynamics and control of open quantum systems, Lecture notes (2015).

[53] H. I. Nurdin, N. Yamamoto, Linear dynamical quantum systems, in: Analysis, Synthesis, and Control, Springer, 2017.

[54] S. Xue, M. R. Hush, I. R. Petersen, Feedback tracking control of non-markovian quantum systems, IEEE Transactions on Control Systems Technology 25 (5) (2017) 1552–1563.

[55] R. Loudon, The Quantum Theory of Light, OUP Oxford, 2000.

[56] D. Roy, C. M. Wilson, O. Firstenberg, Colloquium: Strongly interacting photons in one-dimensional continuum, Reviews of Modern Physics 89 (2) (2017) 021001.

[57] G. Zhang, M. R. James, Direct and indirect couplings in coherent feedback control of linear quantum systems, IEEE Transactions on Automatic Control 56 (2011) 1535–1550.

[58] S. N. Sivanandam, K. Sreekala, An algebraic approach for stability analysis of linear systems with complex coefficients, International Journal of Computer Applications 44 (3) (2012) 13–16.

[59] G. Zhang, S. Grivopoulos, I. R. Petersen, J. E. Gough, The kalman decomposition for linear quantum systems, IEEE Transactions on Automatic Control 63 (2) (2018) 331–346.

[60] N. Yamamoto, Coherent versus measurement feedback: Linear systems theory for quantum information, Physical Review X 4 (2014) 041029.

[61] N. Yamamoto, Decoherence-free linear quantum subsystems, IEEE Transactions on Automatic Control 59 (7) (2014) 1845–1857.

[62] N. Schuch, J. Siewert, Natural two-qubit gate for quantum computation using the XY interaction, Physical Review A 67 (2003) 032301.

[63] Y. Pan, G. Zhang, W. Cui, M. R. James, Single photon inverting pulse for an atom in a cavity, in: 2015 54th IEEE Conference on Decision and Control (CDC), IEEE, 2015, pp. 6429–6433.